IDENTIFYING CHANGES IN MANGROVES IN TRAT PROVINCE, THAILAND AND KOH KONG PROVINCE, CAMBODIA

A Thesis submitted to the faculty of
San Francisco State University
In partial fulfillment of
the requirements for
the Degree

Master of Science

In

Geographic Information Science

by

Rubaya Pervin

San Francisco, California

May 2016

CERTIFICATION OF APPROVAL

I certify that I have read Identifying Changes in Mangroves in Trat Province, Thailand and Koh Kong Province, Cambodia by Rubaya Pervin, and that in my opinion this work meets the criteria for approving a thesis submitted in partial fulfillment of the requirement for the degree Master of Science in Geography: Geographic Information Science at San Francisco State University.

Ellen Hines Ph.D.
Professor,
Dept. of Geography & Environment
San Francisco State University

Leonhard Blesius Ph.D.
Associate Professor,
Dept. of Geography & Environment
San Francisco State University

Claudia Baldwin Ph.D.
Associate Professor,
Environmental and Planning Studies
University of the Sunshine Coast

IDENTIFYING CHANGES IN MANGROVES IN TRAT PROVINCE, THAILAND AND KOH KONG PROVINCE, CAMBODIA

Rubaya Pervin
San Francisco, California
2016

Studies showed that from 1960 to 1996 mangrove forests in Thailand decreased over time due to increasing shrimp cultivation in those areas. Both in Thailand and Cambodia, most of the farms were in the vicinity of mangrove forests and adversely affected the mangrove ecosystem. The focus of this research was to detect changes in the extent of mangroves and other land-use changes along the coastal area of Trat Province, Thailand and Koh Kong Province, Cambodia from 1996 to 2015. Object-oriented Nearest Neighbor classification approach was used to identify mangroves, non-mangrove trees, active shrimp farms, inactive shrimp farms, agricultural fields, and developed areas. The results indicate that mangrove forests decreased from 8% to 33% over time in both of the study areas, with the exception that mangroves increased by 7.7% in Koh Kong Province, Cambodia from 2009 to 2015. Agricultural fields, planted trees, and both active and inactive shrimp farms were primarily seen in place of mangrove areas.

I certify that the Abstract is a correct representation of the content of this thesis.

_____ _____

Chair, Thesis Committee Date

ACKNOWLEDGEMENTS

All praises go to the Almighty Allah for giving me the opportunity and strength to achieve a Master of Science degree.

Foremost, I convey my sincere gratitude to my advisor Prof. Ellen Hines for her guidance and support in my study. She patiently nurtured me and enthusiastically helped me in my research and writing the thesis. I am grateful to Prof. Leonhard Blesius and Prof. Claudia Baldwin for serving in my advising committee and guiding me with their immense knowledge.

I sincerely thank my family for their encouragement and inspiration to pursue higher education abroad.

It has been a great privilege to pursue my master's study in the Department of Geography & Environment at San Francisco State University. I would like to thank the university and the department for providing me an excellent environment for learning and research. I will always cherish my memory at SFSU.

TABLE OF CONTENTS

List of Table vii

List of Figures viii

1 Introduction 1

2 Study areas and data collection 6

2.1 Study area location 6

2.2 Data collection 7

3 Methodology 8

3.1 Image prep-processing 9

3.2 Image segmentation and classification 11

3.3 Accuracy Assessment 16

3.4 Bi-temporal change detection 18

4 Results 19

4.1 Overall changes 19

4.2 The conversion of mangroves into other classes 30

5 Discussion and Conclusions 34

References 37

LIST OF TABLES

Table Page

1. Table 2.1: The bands that were used in this study.....7
2. Table 4.1: Confusion Matrix for accuracy assessment.....20
3. Table 4.2: Percent change in area (in hectares) for each class 29

LIST OF FIGURES

Figure Page

1. Figure 2.1: Study area.…….....6
2. Figure 3.1: Object-oriented classification flow chart.....10
3. Figure 3.2: Final study area for classification.....11
4. Figure 3.3: Segments created by the multi-resolution image segmentation.....13
5. Figure 3.4: A zoomed-in section of the study area after merging classes 16
6. Figure 3.5: Model to identify areas of mangrove conversion.....18
7. Figure 4.1: Percentage of mangrove change between each pair of adjacent time points in the study areas.....21
8. Figure 4.2: Classified study area map of 1996 and 2003.....23
9. Figure 4.3: Classified study area map of 2003 and 2009.....24
10. Figure 4.4: Classified study area map of 2009 and 2015.....25
11. Figure 4.5: Area of highest mangrove deforestation in Trat Province.....26
12. Figure 4.6: Area of highest mangrove deforestation in Koh Kong Province.....27
13. Figure 4.7: Change in area for each land use class in Thailand.....28
14. Figure 4.8: Change in area for each land use class in Cambodia.....29
15. Figure 4.9: Conversion of mangrove area between 1996 and 2003.....31
16. Figure 4.10: Conversion of mangrove area between 2003 and 2009.....31
17. Figure 4.11: Conversion of mangrove area into other land cover/use in Trat Province, Thailand between 2009 and 2015, in percent.....32
18. Figure 4.12: Conversion of other land cover/use into mangroves in Koh Kong Province, Cambodia between 2009 and 2015, in percent.....33

1 INTRODUCTION

Mangrove forests are unique because of their location in regions near seawater, fresh water and coastal lands. The unique environment of sea and land combinations creates sanctuaries, nurseries and habitat for marine life (Kathiresan & Bingham, 2001, Lugendo et al., 2007; Madren, 2012). Mangrove forests are some of the most productive and biologically diverse ecosystems in the world. For example, this diverse ecosystem has about 80 different tree species. Mangrove forests particularly inhabit tropical and subtropical regions and protect coastal areas by reducing the wave energy of tsunamis, hurricanes and storm surges. The effect of the 2004 tsunami in Southeast Asia might not have been so devastating if there had been a healthy mangrove coastline to reduce the intensity of the tidal surge (Kathiresan & Bingham, 2001, Madren, 2012). Total mangrove forest areas of the world are distributed over 118 countries and among them 42 percent are located in Asia (Giri *et al.,* 2011). This research investigated mangrove distribution changes in two countries in Southeast Asia.

Southeast Asia has 35% of the world's mangrove areas. However, in the last few decades, these mangroves are decreasing at an alarming rate. Human induced activities and natural changes influence the devastation of mangroves (Nguyen *et al.,* 2013). Agricultural expansion (81%), aquaculture (12%) and urban development (2%) are the main reasons behind mangrove deforestation in the Asian region. However, the scale of changes in land-use and other related factors that cause mangrove deforestation vary from

one region to another. For each Southeast Asian country, human activities, especially shrimp farming and agriculture, strongly drive mangrove deforestation (Nguyen *et al.,* 2013). In Thailand, main drivers of mangrove deforestation are agriculture (50%), aquaculture (41%) and urban development (2%) (Giri *et al*., 2008). Therefore, this research compared and contrasted mangrove deforestation and other land use changes in different regions of two Southeast Asian countries, Trat Province in Thailand and adjacent Koh Kong Province in Cambodia.

Thailand is an extreme example of mangrove deforestation. One of the main causes of this problem is shrimp farming, which significantly affects the extent of mangrove deforestation. Approximately one third of the mangrove deforestation from 1960 to 1996 was caused by shrimp farms (Aksornkoae & Tokrisna, 2004; Naito & Traesupap, 2006). However, the effect of shrimp farming on mangrove deforestation varies significantly depending on the timeframe and scale of the study. For example, a recent study in 2014 showed only a moderate exploitation of mangroves from 1989 to 2007 at village level in three villages of Krabi Province, Thailand. (Peneva-Reed, 2014).

Thailand's shrimp industry started an unprecedented expansion in 1987 with the collapse of the then leading shrimp farming industry in Taiwan. The collapse in Taiwan was initiated by pollution, disease, over-stocking, over-exploitation of groundwater. Thailand responded quickly to grab the market and became a leading exporter of cultured shrimp and tiger prawns. In this process, the number of farms in Thailand grew rapidly, of which

85% were intensive (Huitric *et al.,* 2002). In Cambodia, intensive commercial shrimp farming is mainly located in the Koh Kong Province near Thailand. Aquaculture in Koh Kong Province flourished in 1994, but an outbreak of diseases forced 80 percent of the intensive farms to cease operation by 2004. Koh Kong Province has the vast magnitude of mangroves in Cambodia (Bann, 1997; Song *et al*., 2004).

Both in Thailand and Cambodia, most of these intensive farms were in the vicinity of mangrove forests. As a result, the mangrove ecosystem was severely affected by farm waste and other chemicals used in the farming as well as the construction of new infrastructure needed by shrimp industry such as roads or dams. Shrimp farmers often made these degradations permanent by deforestation and constructing new infrastructure. This process continued over time as more and more forest areas were occupied by farms and related developments, eventually displacing a significant part of existing mangrove forests. Even a national ban on logging in mangroves in 1996 could not prevent the widespread mangrove destruction (Huitric *et al.,* 2002; Thongrak *et al.,* 1997).

Landsat imagery and other satellite images are commonly used in mangrove identification and change detection (Giri *et al*., 2008; Giri *et al*., 2011; Beh *et al.,* 2012; Nguyen *et al.,* 2013). Landsat images are also used in small scale local or village level mangrove change detection. It is common to identify shrimp farms and other land-use changes with Landsat images (Peneva-Reed, 2014; Nguyen, 2014). Therefore, this

research used Landsat images to identify mangroves and other land-use and land-cover changes with a change detection method.

Change detection techniques use multi-temporal imagery to derive timely information on the earth's environment and human activities (Jianya *et al.,* 2008). It is a complicated and integrated process, and there is no existing approach that is optimal and applicable to all cases. Change detection approaches are characterized into two broad groups: bi-temporal change detection and temporal trajectory analysis. Bi-temporal image change detection is a method where two images of the same location at different time points were compared to identify changes. By contrast, trajectory analysis compares larger number of images from a series of time points to identify change trajectories of an individual land cover class at the same location. The latter method is mostly based on high temporal resolution and low spatial resolution images (Jianya *et al.,* 2008). In trajectory analysis, classification is very difficult due to the use of images with lower spatial details. Since we are interested in changes of several land-cover and land-use classes at different time points, we used bi-temporal change detection techniques. For this purpose, we detect changes after the images are independently classified beforehand, a technique know as post-classification change detection (Singh, 1989). Previous work found post-classification comparison to be the most accurate procedure for Landsat images (Mas, 1999). Furthermore, it has the advantage of indicating the nature of the changes in different classes. These advantages motivated us to use post-classification bi-temporal change detection techniques.

Bi-temporal change detection is important to environment changes at different scales and is used to analyze the impact of human activities on environmental elements (Jianya *et al.,* 2008). Identifying the areas of highest mangrove change and understanding the drivers of mangrove devastation can assist coastal decision and policy makers to reduce further deforestation of mangroves for vulnerable coastal areas (Beh *et al.,* 2012; Nguyen *et al.,* 2013). GIS and remote sensing change detection can assist decision and policy makers to identify the drivers of mangrove deforestation (Giri *et al.,* 2011). This research detected mangrove deforestation and the conversion of mangroves into other land uses that can be identified as human induced drivers of mangrove deterioration such as shrimp farming and agricultural activities.

2 STUDY AREAS AND DATA COLLECTION

2.1 Study area location

The research covers the coastal area of Trat Province, Thailand and Koh Kong Province, Cambodia. Figure 2.1 presents the study area from a global perspective (left) and the overall study area (right).

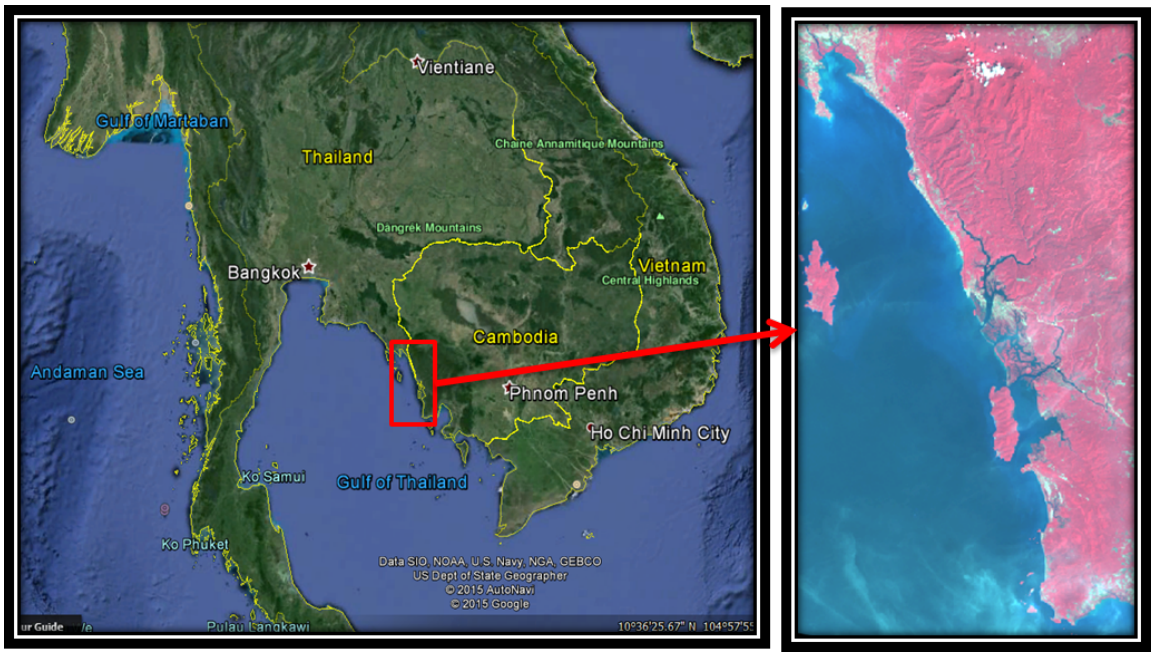

Figure 2.1: Study area. Left: From a global perspective; Right: The overall study area. (Image source: Left: Google earth, Right: http://glovis.usgs.gov/)

2.2 Data collection

Four Landsat scenes of the Thailand and Cambodia coastline were used. The images were from Landsat 5 on January 1996 and 2009, Landsat 7 on January 2003, and Landsat 8 on February 2015. All images were taken between 9:30am to 10:30 am local time for Thailand and Cambodia. In ERDAS Imagine (Version 14), the desired maps were created for 1996, 2003, 2009 and 2015 by stacking the layers shown in Table 2.1. Finally, we created subsets for the overall study location (the right image in Figure 2.1). We stacked thermal bands for Landsat 5 and Landsat 7 images. For our specific Landsat 8 image, the thermal band was not showing any values. Therefore, the Landsat 8 thermal bands were not included.

Table 2.1: The bands that were used in this study

Bands	Landsat 5	Landsat 7	Landsat 8
Band 1	Blue	Blue	Coastal
Band 2	Green	Green	Blue
Band 3	Red	Red	Green
Band 4	NIR	NIR	Red
Band 5	SWIR-1	SWIR-1	NIR
Band 6	TIR	TIR	SWIR-1
Band 7	SWIR-2	SWIR-2	SWIR-2

3 METHODOLOGY

This research focuses on local scale mangrove change detection and the detection of how land-use and land-cover changes modify patterns of mangroves in the coastal environment. When our objective is to identify land-use and land-cover changes, it is preferable to detect changes in classified images (El-Kawy *et al*., 2011). In this research, we used by-temporal change detection in images classified by object-oriented classification. Object-oriented classification identifies and classifies image domain as objects based on spectral and spatial information (Blaschke *et al.*, 2000). Object-oriented spectral classification with a nearest neighbor (NN) classifier has been used successfully for many classification problems (Leckie *et al.,* 2005; Conchedda *et. al.,* 2008). Object based classification creates homogeneous natural looking classes. It does not show any salt and pepper effect (single pixels are classified differently than the surrounding homogeneous area) (Blaschke *et al.*, 2000). Object based classification has been shown to achieve higher accuracy compared to pixel based classification (Myint *et. al*., 2008). Furthermore, several classes considered in this research such as shrimp farms and agricultural fields are naturally distinguishable objects. Therefore, this research used object-oriented spectral classification with a nearest neighbor (NN) classification method for post-classification change detection. NN is a supervised classification approach. For each of the classes, training samples were collected from known image segments to classify all remaining (unknown) objects in the image.

Figure 3.1 shows the two steps involved in the change detection method used in this research. First, we classified images with object-oriented image classification. Second, bi-temporal image change detection were used for post classification change detection. The top part of Figure 3.1 elaborates key steps of the classification method with a flow chart. After preprocessing an image to eliminate atmospheric effects, we segmented the image where each segment represents a group of homogeneous pixels at a given resolution. These segments were used as objects in an object oriented-oriented classification. Finally, neighboring segments from the same class were merged and exported as the final classification result. These steps are discussed in more detail in later subsections. We applied this procedure to each of the four Landsat images separately. Once we created the class hierarchy and processed tree of the following chart, it was applied to each image. However, for every image, new training samples were collected.

3.1 Image pre-processing

Before classifying the images, atmospheric effects on the images were attenuated. For haze correction and atmospheric corrections, we used ATCOR2 workstation (an add-on module to ERDAS IMAGINE for atmospheric correction for professionals for flat terrain) and ERDAS model maker (Version 14). Using the ATCOR2 workstation, we resampled the coarser thermal layers to the 30 m resolution of the finer image layers and calculated surface temperature from the thermal band. However, we were unable to use Landsat 8 thermal band because ATCOR2 currently does not support it.

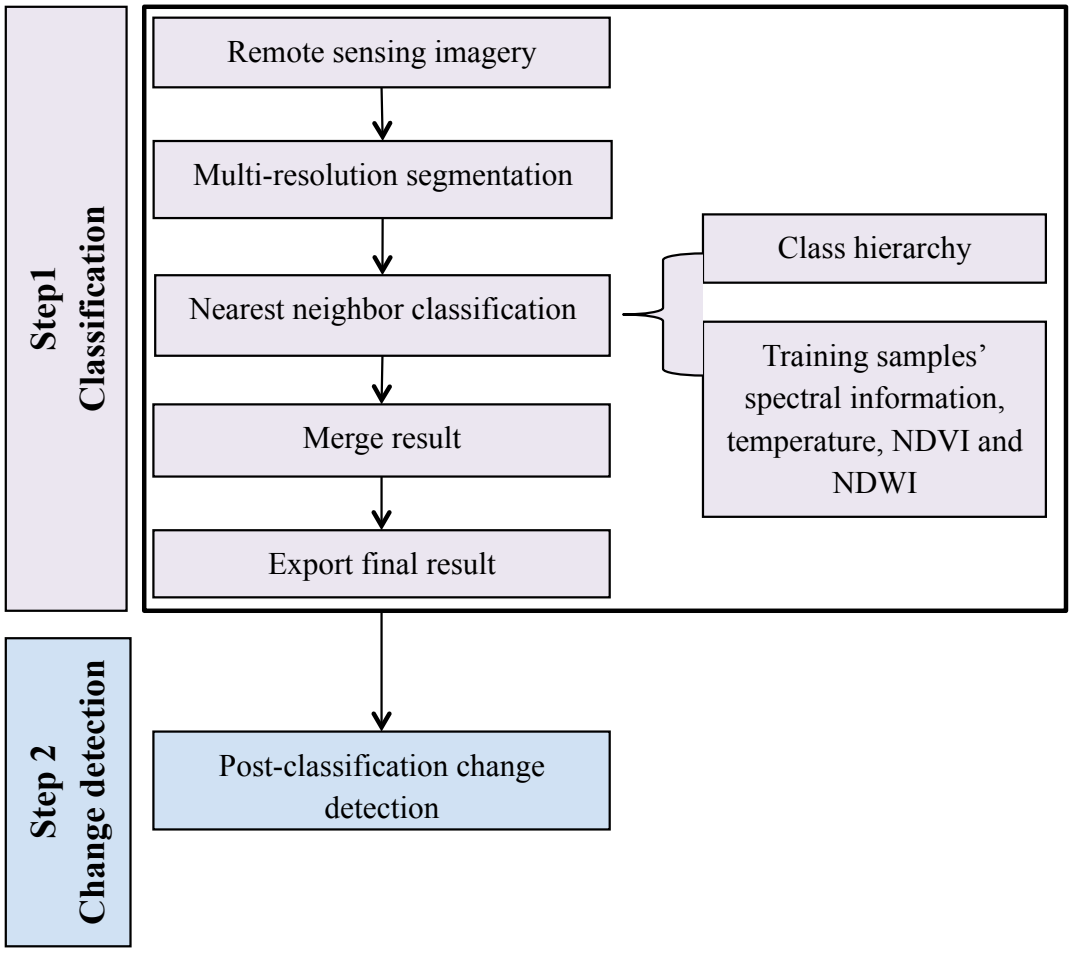

Figure 3.1: Object-oriented classification flow chart shows steps used in this research

Since this research focused on mangrove changes and the effect of other land-use changes on mangroves, we only considered the areas with mangrove coverage. A 3 km buffer zone from the coastline covers almost all mangroves on the overall study area. Therefore, to mask out only the specific area of interest along the coast, we used a

geographic information system (GIS) to create a mask raster. Figure 3.2 shows the study area extent for the 2015 image.

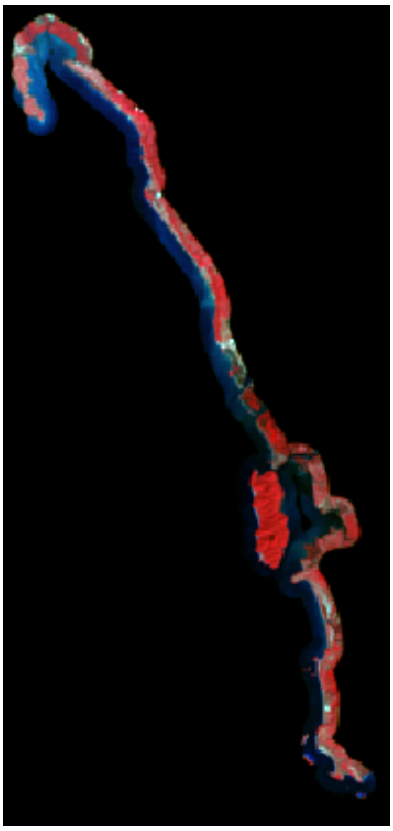

Figure 3.2: Final study area for classification

3.2 Image segmentation and classification

Image segmentation

Image segmentation creates homogeneous image objects for further classification. For remote sensing image analysis, numerous image segmentation algorithms can be applied to create homogeneous segments (Blaschke *et. al*., 2000; Dey *et. al.,* 2010). For many

applications, segmentation needs to be combined at different scale levels for different meaningful objects. For this purpose, eCognition software has developed a multi-resolution image segmentation process that is frequently used in remote sensing applications (Benz *et. al*., 2004, Blaschke, 2010). The multi-resolution image segmentation used in eCognition is a bottom up region-merging technique starting with one-pixel objects. In subsequent steps, smaller image objects are merged into bigger ones in a hierarchical fashion. The merging process stops when the segments become homogeneous. Since identifying shrimp farms, that are usually square or rectangular, is one of our primary objectives, we considered image shape to be an important part during segmentation. Therefore, shape was given a higher weight during segmentation. For multi-resolution segmentation, the shape parameter was given a weightage of 0.2 (default shape parameter is 0.1) and compactness was set to its default value of 0.5. Scale parameters were 8 for the 1996, 2003 and 2009 images and 60 for the 2015 image. These values are chosen by trial and error with an emphasis on better identification of individual shrimp farms. See Figure 3.3 for an example of the image objects created from multi-resolution image segmentation.

Classification

For classification purposes, first we set up the class hierarchy. Next, we collected our training samples from known segmentations, and then executed the classification. Based

on preliminary investigation of the area on Google Earth, we detected seven classes for land-cover and land-use on our research sites. These classes are (1) mangroves, (2) non-

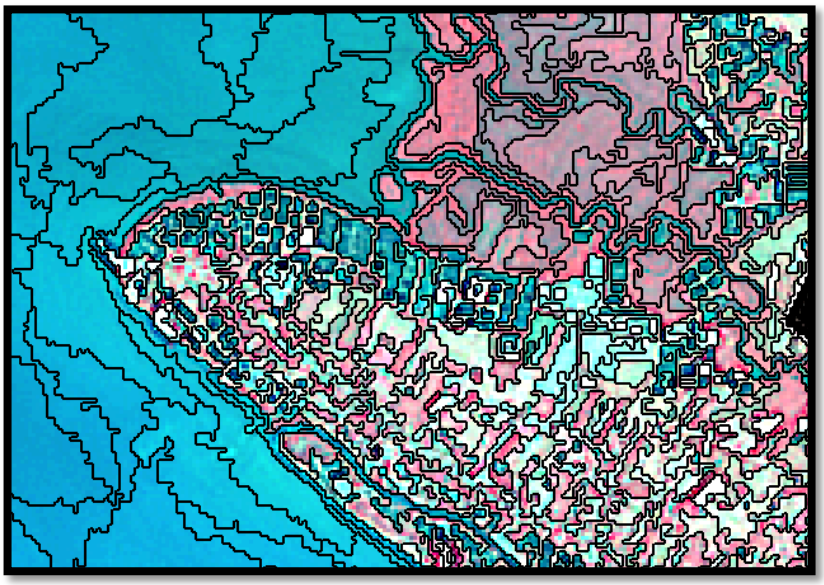

Figure 3.3: Segments created by the multi-resolution image segmentation process.

mangrove trees, (3) active shrimp farms, (4) inactive shrimp farms, (5) agricultural fields and planted trees, (6) developed areas and barren lands, and (7) water. Active shrimp farms have water layers and therefore have similar spectral responses as water. The class "inactive shrimp farms" represents the dried-out shrimp farms. Planted trees on the study area were difficult to identify at the 30 meter resolution of Landsat images. Therefore, most of the planted trees were included in the "agricultural fields and planted trees" class. The "developed areas and bare grounds" class included all types of developed areas and open grounds due to similar spectral responses.

Image object parameters such as mean object spectral responses, brightness, MaxDiff, temperature, normalized difference vegetation index (NDVI), normalized difference water index (NDWI) were inserted for the standard nearest neighbor algorithm. All parameters helped to identify the classes, especially the NDVI, which helped to better identify the mangroves, non mangroves, agricultural fields and planted trees. Vegetation canopies have lower reflectance in red (because of chlorophyll absorption) and have very high reflectance in near-infrared. Equation 1 calculates NDVI values in range between -1 to +1, where a negative value denotes non-vegetation and a positive value denotes vegetation (Gao, 1996). Green vegetation has higher positive NDVI value with mangroves having the highest NDVI value.

$$NDVI = \frac{NIR - \mathrm{Re}d}{NIR + \mathrm{Re}d} \tag{1}$$

The NDWI helped to better identify the shrimp farms and water. NDWI were calculated based on following equations.

$$NDWI = \frac{Green - NIR}{Green + NIR} \tag{2}$$

NDWI can be calculated based on either SWIR (shortwave infrared) band or the green band. NDWI calculated from these two different bands has different applications. NDWI based on SWIR is primarily used to identify vegetation water content (Gao, 1996; Jackson *et. al.,* 2004). By contrast, NDWI based on the green band has been used to

identify surface water features (Ji *et. al.*, 2009; McFeeters, 1996). Therefore, the green band based NDWI is more appropriate to distinguish shrimp farms from water in the classification.

Inactive shrimp farms are difficult to differentiate from developed areas due to the similarity in their spectral responses. However, the existence of more impervious surfaces in developed areas gives rise to higher temperature than inactive shrimp farms. Therefore, the thermal signature helped to distinguish these two classes.

Google Earth was used to identify the location of classes when selecting training samples. For the pixel-based classification, the number training samples for each class is suggested to be 10-30 times the number of bands (Niel *et. al*., 2005). However, object oriented classification has no accepted guideline for selecting the number of training samples. Generally, classification accuracy increases with the increase of training samples. However, increasing the sample size above 125 does not improve the accuracy significantly (Qian 2014). Each of the seven classes in our classification has the number of training samples between 18-125. The classes that cover smaller map area (i.e. inactive shrimp farms, active shrimp farms) had smaller sample sizes and larger classes had greater number of samples. For 2015 image classification, the larger classes (e.g., non mangroves) had more than 125 training samples. The total number of samples ranges 2-5% of the image objects. These training samples were selected from known areas and distributed uniformly at random over the image area.

Classification was executed based on the information of NN parameters of the training samples. After classification, the segments were merged so that all neighboring objects of the same class formed single objects. Figure 3.4 represents the section of the study area shown in Figure 3.3 after merging classes.

Figure 3.4: A zoomed-in section of the study area from Figure 3.3 after merging classes.

The last step was to export the classification result into a vector layer and create classification maps using the exported vector layers.

3.3 Accuracy Assessment

For an accuracy assessment, we used an ArcGIS base map, which is a 1m resolution Ikonos satellite image obtained in 2009. Therefore, the accuracy assessment was conducted on the 2009 Landsat image. Due to the unavailability of high-resolution

reference images, accuracy assessments for 1996, 2003 and 2015 images were not conducted.

To determine the appropriate sample size, we used the following multinomial distribution equation (Congalton and Green, 2008)

$$N = \frac{B\Pi_i(1-\Pi_i)}{b_i^2} \quad (3)$$

where, N is sample size, $\prod_i$ is proportion of class closest to the map area, B is upper (α/number of classes) percentile of chi-square distribution with 1 degree of freedom, and b_i is precision (e.g. 5% error, i.e. 95% confidence limit).

In this research, our classification process had seven categories. When a the largest class makes up an estimated 25% of the map area at a 95% confidence level or 5% precision, using the above equation, the desired sample size is 543. Five hundred and forty-three randomly distributed points were used to estimate the classification accuracy. A confusion matrix (also known as an error matrix) was created to calculate errors of omission, commission and overall accuracy based on the 543 points.

3.4 Bi-temporal change detection

For bi-temporal change detection, we compared a pair of images of the same location (either Trat Province or Koh Kong Province) taken at two different time points. In Figure 3.5, we compared the image of an area at a given time (i.e. Trat Province 1996) as an

unchanged input and an image of the same area at a different time (i.e. Trat Province 2003) as a changed image. From this comparison, we could identify how the areas belonging to the same class changed from one time to another. For example, we identified the areas classified as mangroves in the first image of the pair of images under consideration. The same areas were also extracted from the second image. The extracted areas from these two images were then compared to identify the conversion of mangroves into other classes from the first time point to the second time point. A model (Figure 3.5) was created in these analyses so that areas of mangrove conversion into other classes can be automatically calculated by changing the input images.

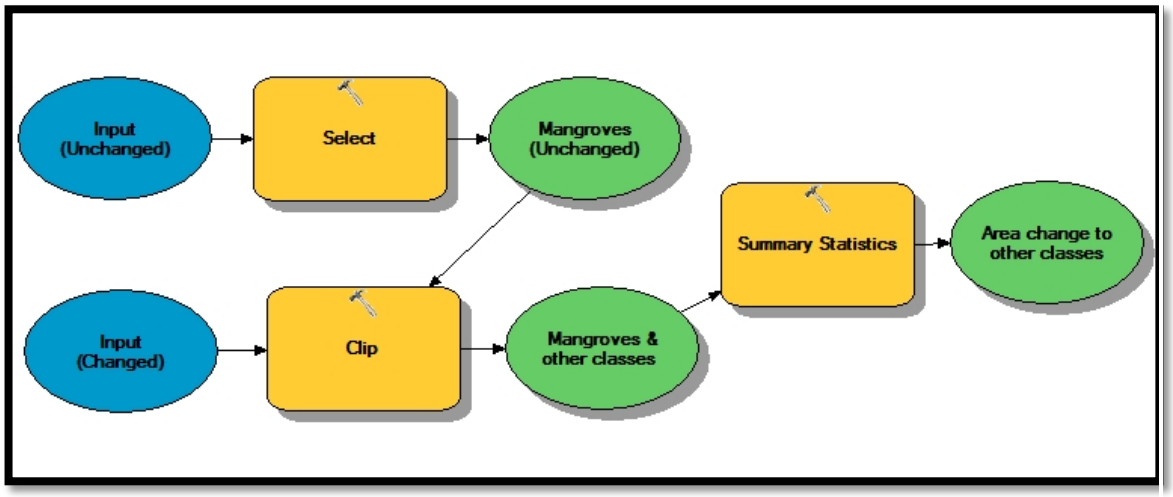

Figure 3.5: Model to identify areas of mangrove conversion into other classes

4 RESULTS

The accuracy evaluation showed that the overall accuracy of the Landsat 2009 image classification was 86.74% at a 95% confidence interval. Table 4.1 shows user accuracy and producer accuracy of the classes. "User's accuracy" presents the reliability of the classification. It indicates the probability of an object classified on the image actually represents that category on the ground (Congalton, 1991). 91.92% user accuracy of mangroves indicates that the class mangrove represents 91.92% of actual mangroves on the ground (Table 4.1). On the other hand, producer accuracy indicates how well total area in a category from the reference data is presented on the classified map/image (Congalton, 1991). Producer accuracy of mangrove in table 4.1 shows that 80.53% mangroves on reference data are correctly classified as mangroves.

4.1 Overall changes

We investigated overall mangrove and other land-use changes in Trat Province and Koh Kong Province for last twenty years from 1996 to 2015. We considered four images taken at approximately equidistant time points (1996, 2003, 2009, 2015) over the study period. By comparing classified images from two adjacent time points, we identified the areas where mangroves changed the most in both geographic locations. The pairwise changes are then aggregated together to discover the trend of change in mangroves over the past twenty years.

Table 4.1: Confusion Matrix for accuracy assessment

Classified image	Reference image								
	Active shrimp farms	Agricultural field & planted trees	Developed & other areas	Inactive shrimp farms	Mangrove	Non Mangrove Trees	Water	Total	Producer Accuracy
Active shrimp farms	19	1	2	1	1	0	2	26	73.08
Agricultural fields and planted trees	0	46	5	0	2	9	0	62	74.19
Developed & other areas	1	2	30	3	2	4	0	42	71.43
Inactive shrimp farms	0	0	5	10	0	1	1	17	58.82
Mangroves	0	2	1	0	91	4	1	99	91.92
Non Mangrove Trees	0	1	2	1	16	197	0	217	90.78
Water	1	0	0	0	1	0	78	80	97.50
Total	21	52	45	15	113	215	82	543	
User Accuracy	90.48	88.46	66.67	66.67	80.53	91.63	100		

Figure 4.1 summarizes the percentage of mangrove change between each pair of adjacent time points in the study areas. In every six year time interval, mangroves decreased in both study areas except between 2009 and 2015 in Cambodia. We created the summary Figure 4.1 from the four classified images. In Figures 4.2, 4.3, and 4.4, we compare pairs of successive images after they are classified and identify the areas that went through the most significant changes. Next, we focused on the areas of the highest changes and show the progression of mangrove deforestation in Figure 4.5 for Trat Province, Thailand and Figure 4.6 for Koh Kong Province, Cambodia.

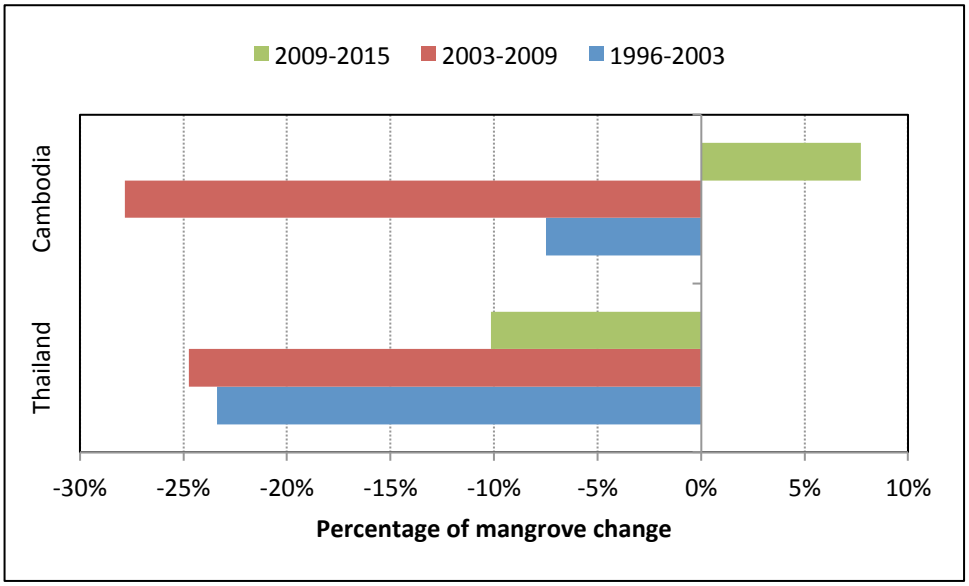

Figure 4.1: Percentage of mangrove change between each pair of adjacent time points in the study areas.

Figure 4.2 shows the classified images of Trat Province, Thailand and Koh Kong Province, Cambodia in the years 1996 and 2003. Figure 4.2(a) shows seven classes in different colors and uses red, black and blue boxes to denote the areas that changed the most from 1996 to 2003. The red box shows the area with the highest change in Thailand, whereas the black and blue boxes mark significant changes in Cambodia. Figure 4.2(b) presents zoomed-in views of these selected regions revealing that while in Thailand mangrove areas in 1996 were primarily replaced by agricultural fields and planted trees in 2003, mangroves in Cambodia were replaced by active shrimp farms and non-mangrove trees, respectively.

Similar to Figure 4.2, Figure 4.3 compares the images from 2003 and 2009, and Figure 4.4 compares classified images from 2009 and 2015. Unlike Figure 4.2, Figure 4.3 and 4.4 show two areas that went through major changes: a red box for Thailand and a black box for Cambodia. These figures demonstrate that mangroves in both study areas decreased over time except in Cambodia from 2009 to 2015. We will describe the amount of mangrove deforestation in more detail in later subsections.

We now focus on the areas where we observed the most severe mangrove deforestation over the years. Figure 4.5 shows the progression of change in the area of greatest mangrove deforestation in Trat Province, Thailand, where mangroves were primarily replaced by agricultural fields and planted trees. This change happened mostly between 1996 and 2003.

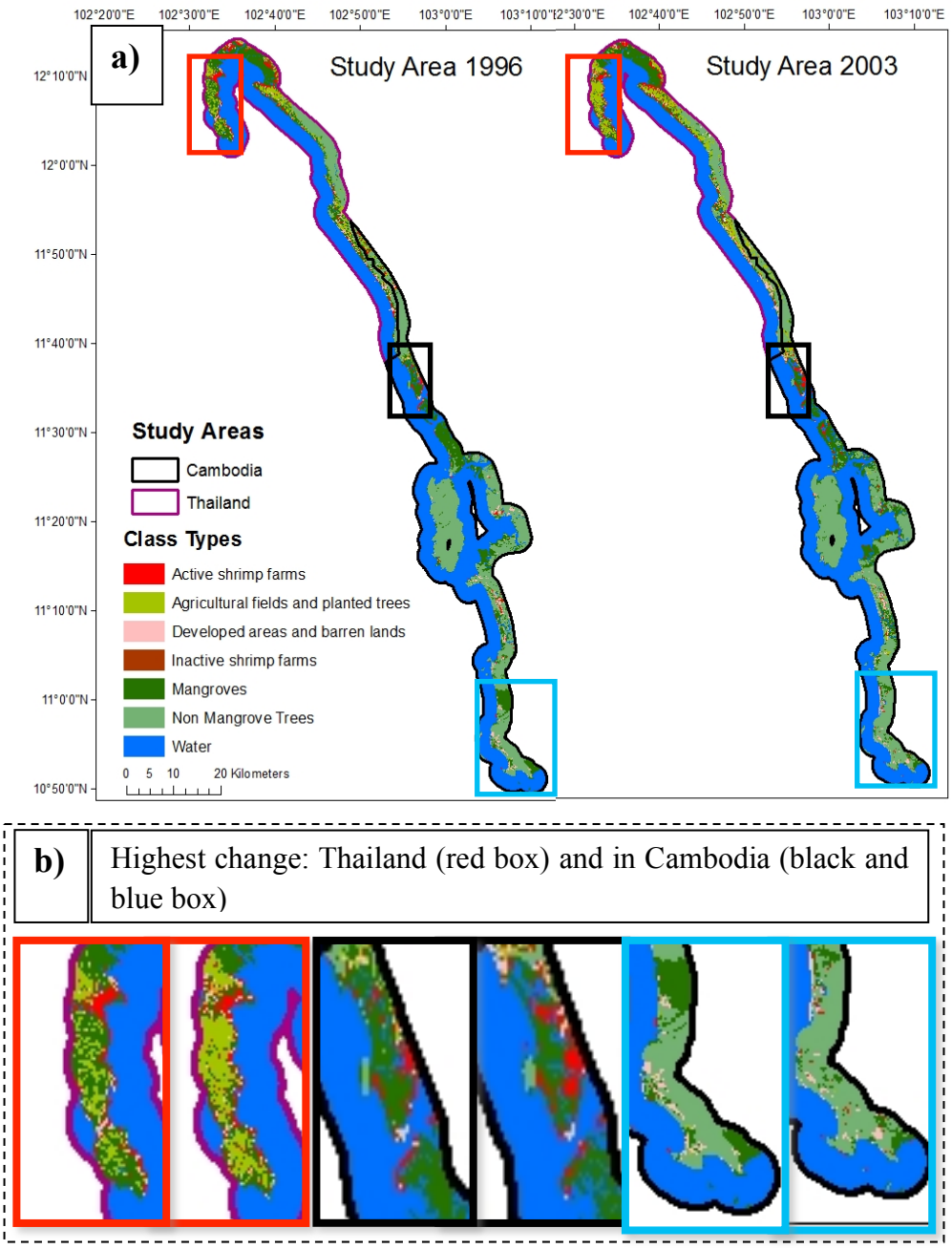

Figure 4.2: (a) Classified study area map of 1996 and 2003 and (b) Highest changes in Thailand (red box) and in Cambodia (black and blue boxes)

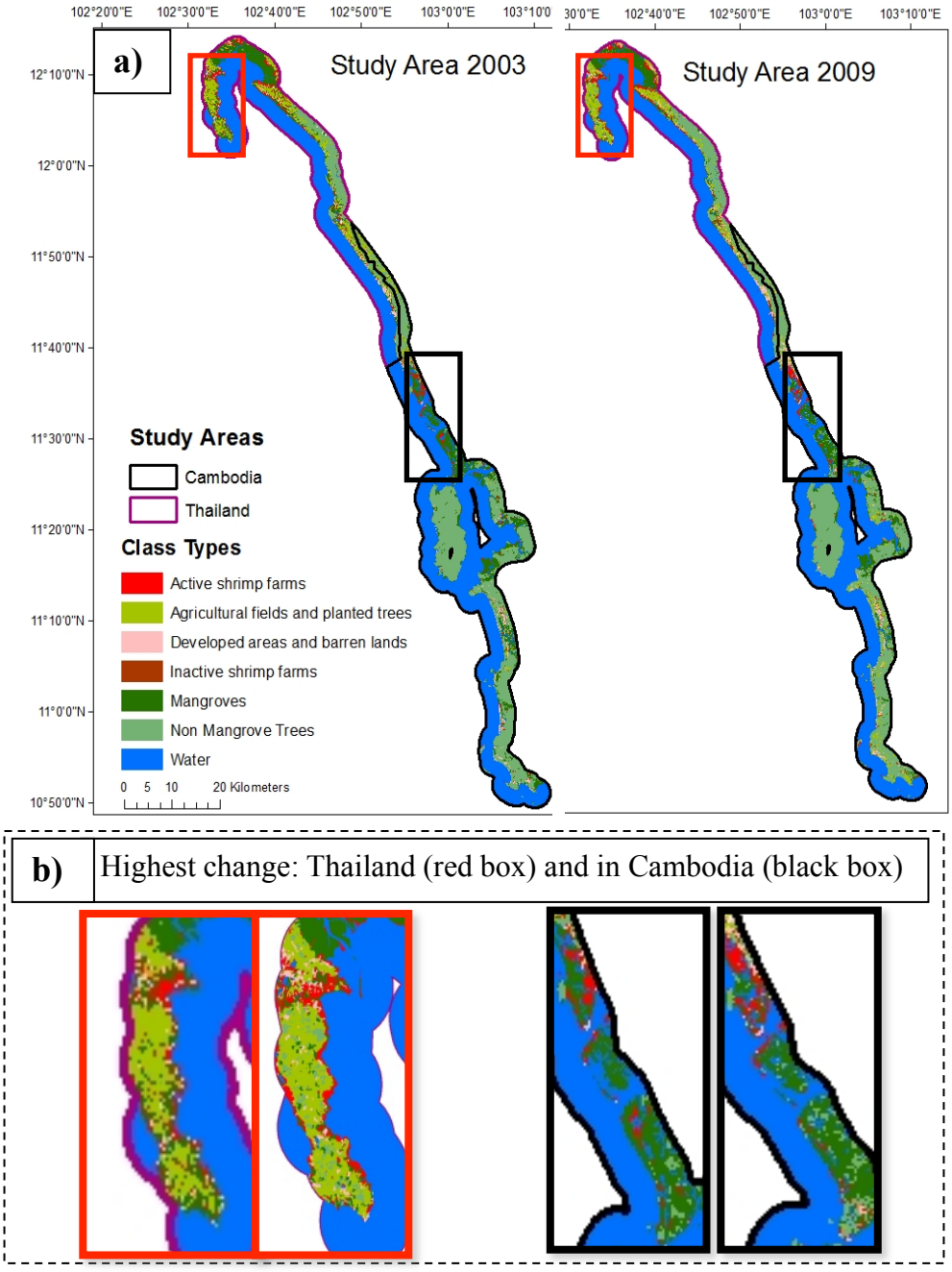

Figure 4.3: (a) Classified study area map of 2003 and 2009 (b) Highest changes in Thailand (red box) and in Cambodia (black boxes)

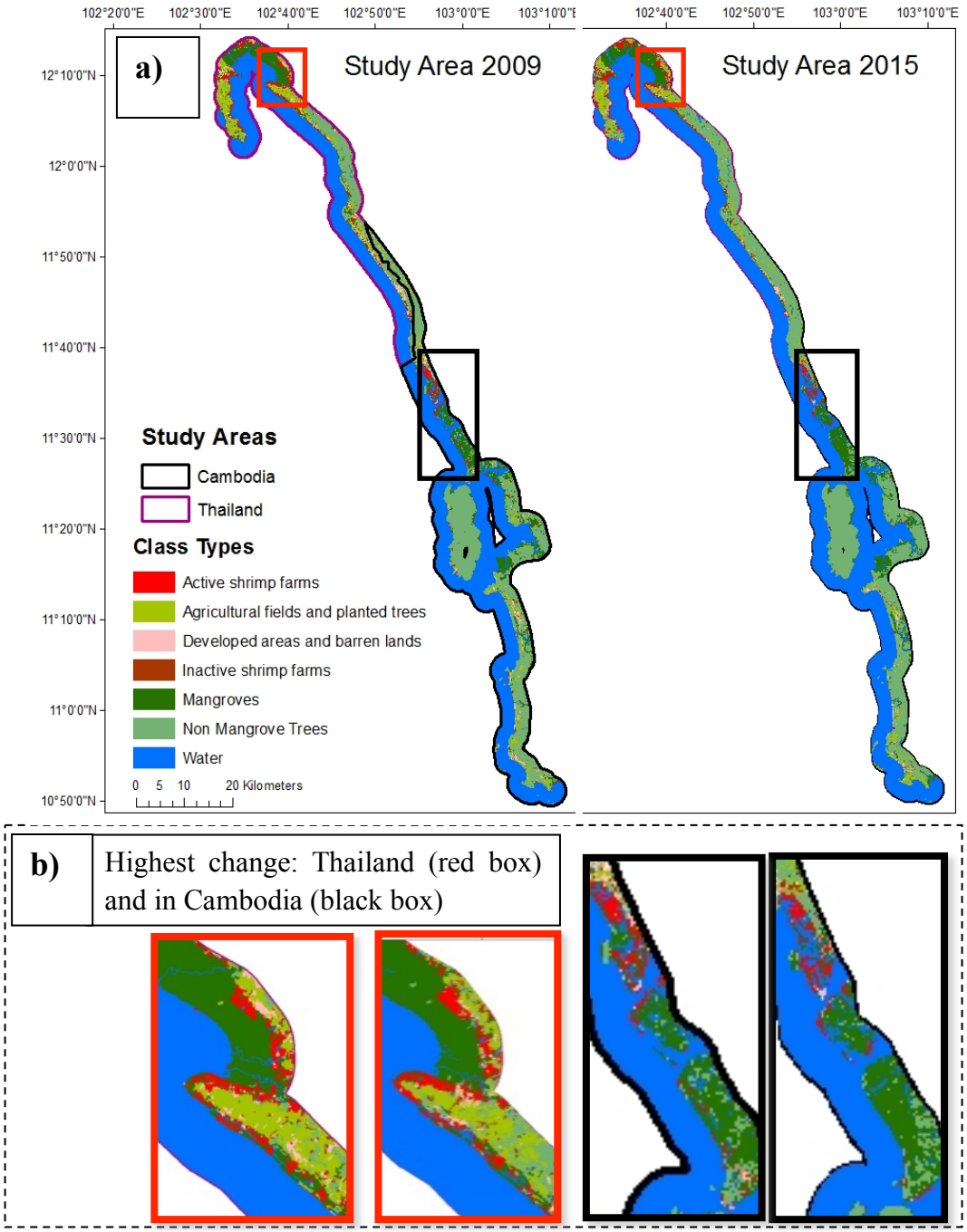

Figure 4.4: (a) Classified study area map of 2009 and 2015 (b) Highest changes in Thailand (red box) and in Cambodia (black boxes)

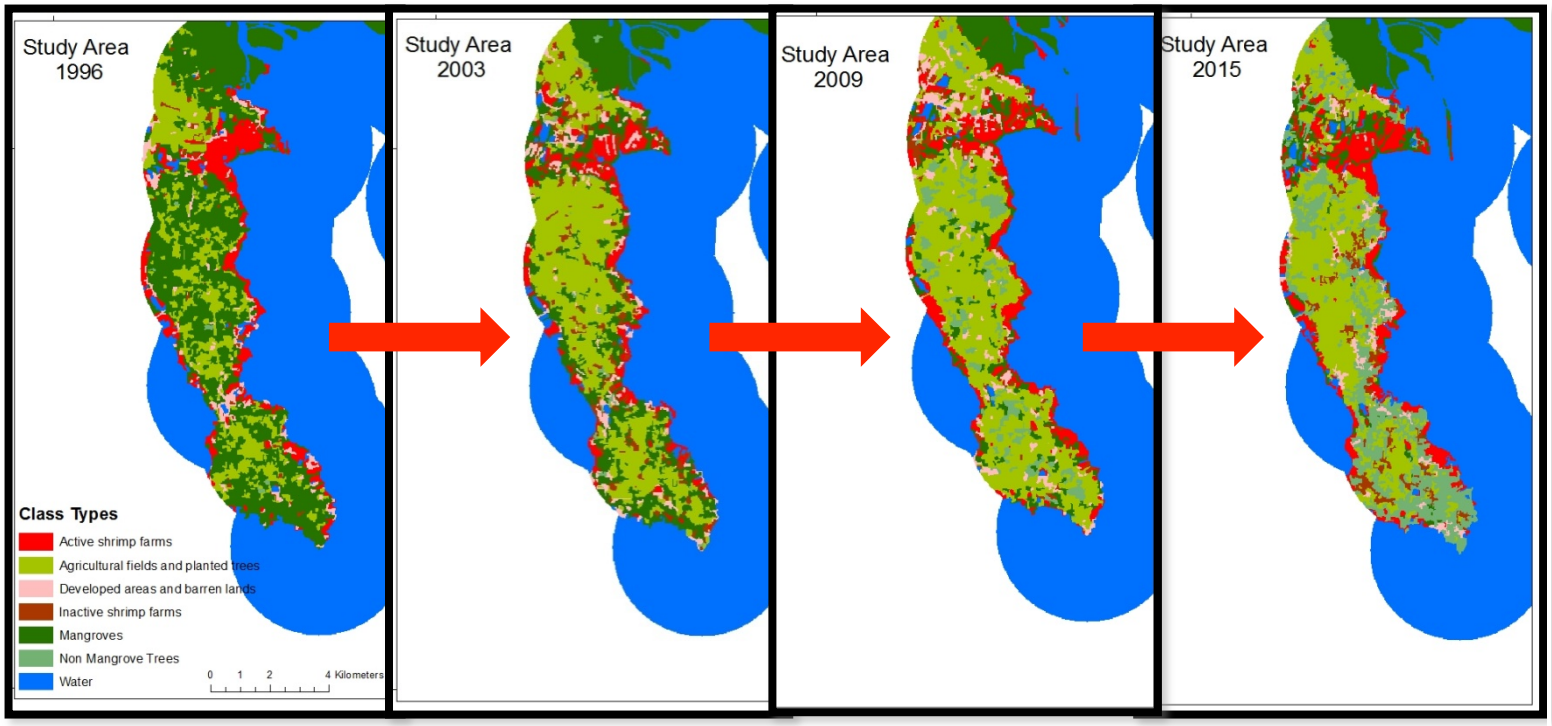

Figure 4.5: Area of highest mangrove deforestation in Trat Province, Thailand, 1996 to 2015

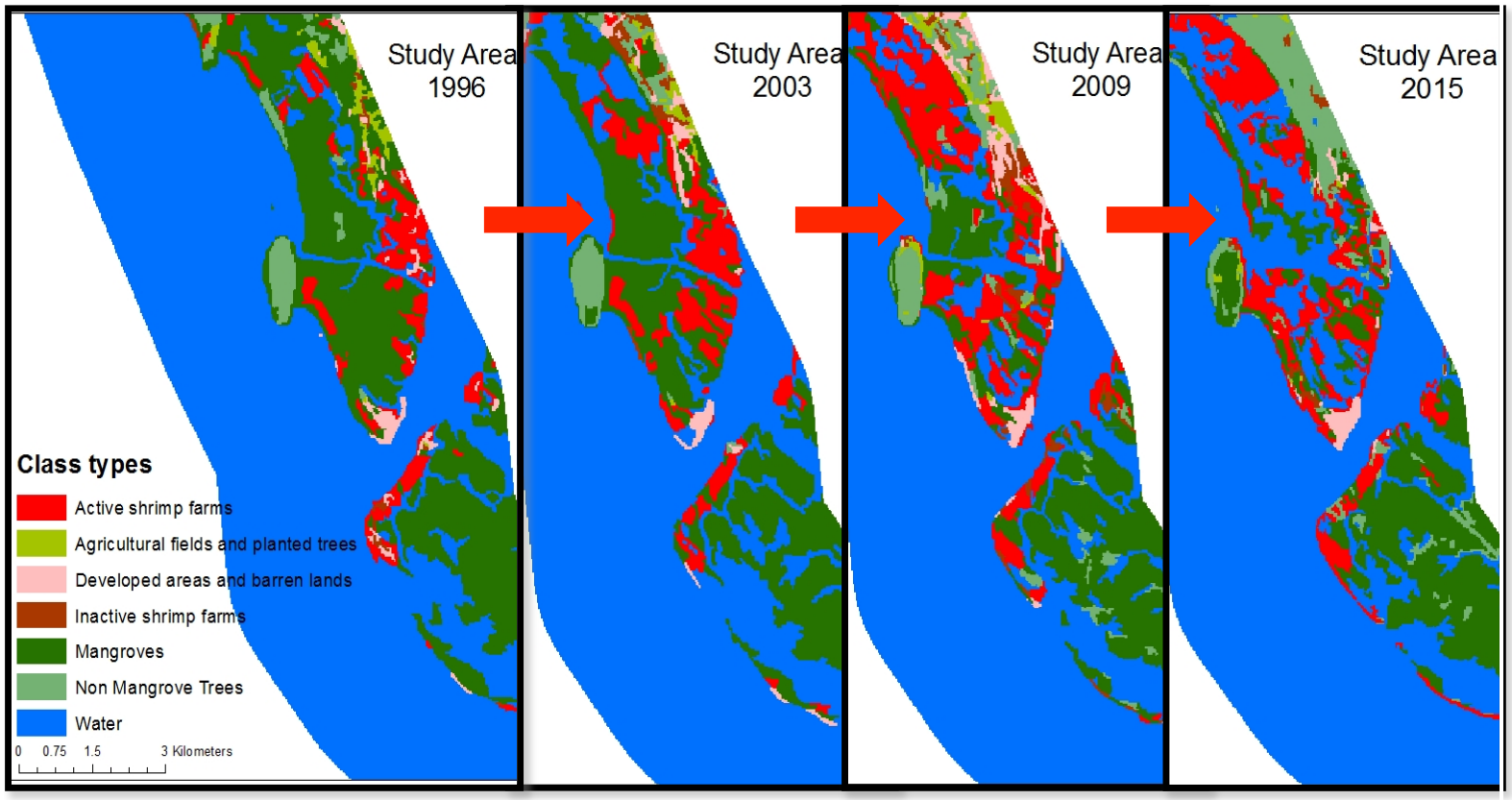

Figure 4.6: Area of highest mangrove deforestation in Koh Kong Province, Cambodia, 1996 to 2015

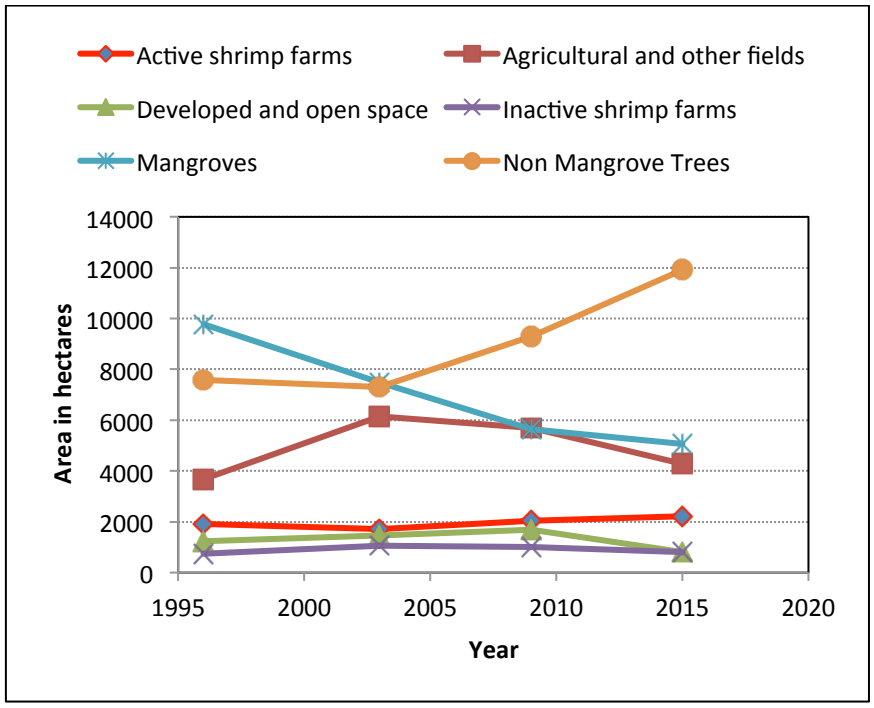

Figure 4.7: Change in area for each land use class in Thailand from 1996 to 2015.

Figure 4.6 shows the progression of change in the greatest area of mangrove deforestation in Koh Kong Province, Cambodia. In contrast to Trat Province, the primary driver of mangrove deforestation in the selected region of Koh Kong Province was active shrimp farming.

Figure 4.7 and Figure 4.8 show how the areas occupied by different classes in Trat Province, Thailand and Koh Kong Province Cambodia changed from 1996 to 2015. These figures demonstrate that mangroves decreased over time in both study areas. In Thailand, the rate of mangrove deforestation was steady from 1996 to 2009, but it slowed

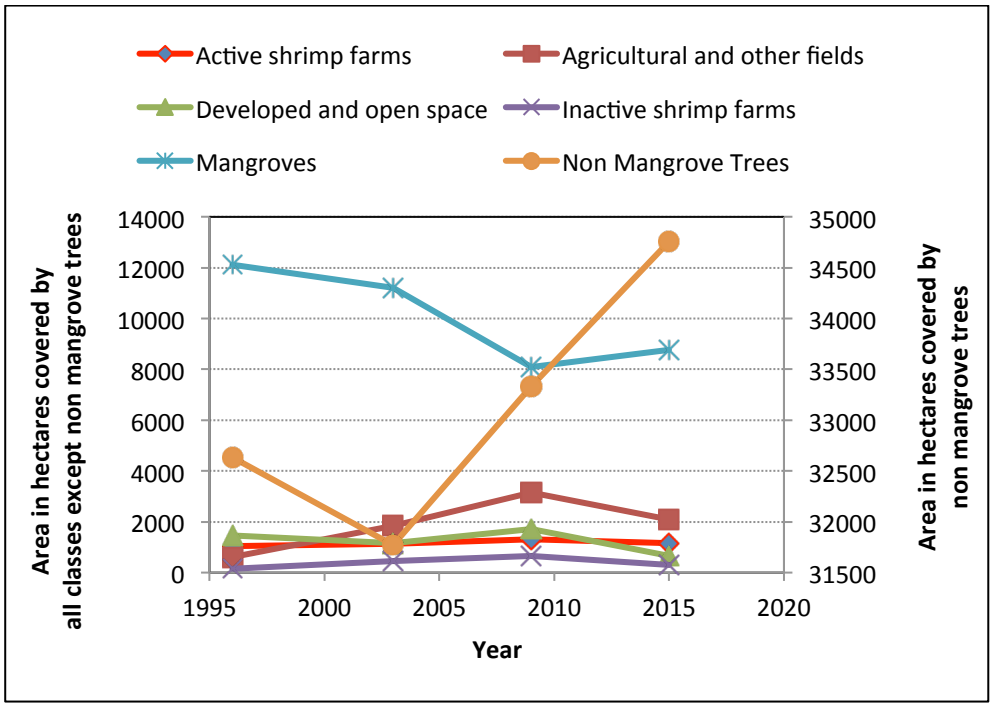

Figure 4.8: Change in area for each land use class in Cambodia from 1996 to 2015

Table 4.2: Percent change in area (in hectares) for each class in Thailand and Cambodia from 1996 to 2015

Classification type	Thailand			Cambodia		
	1996-2003	2003-2009	2009-2015	1996-2003	2003-2009	2009-2015
Active shrimp farms	-12.27	16.49	7.80	8.75	12.72	-11.66
Agricultural fields	40.18	-8.14	-24.43	66.90	41.17	-33.33
Developed and barren areas	15.61	13.96	-52.47	-26.06	32.02	-61.51
Inactive shrimp farms	29.03	-3.56	-19.87	69.60	29.24	-55.22
Mangroves	-30.50	-32.88	-10.14	-8.09	-38.56	7.70
Non Mangrove Trees	-3.78	21.39	22.06	-2.73	4.70	4.09

down between 2009 and 2015. By contrast, in Cambodia, major deforestation of mangroves occurred from 2003 to 2009. From 2009 to 2015, mangrove forests grew over time. Other classes have also changed (either increased or decreased) over the considered time period. The details of all examined changes are given in Table 4.2.

4.2 The conversion of mangroves into other classes

In this subsection, we investigate the primary contributors to mangrove deforestation in our study areas. For this purpose, we observe how mangroves in one image change to other classes in subsequent images. Figure 4.9 shows two pie charts showing the percentage area occupied by mangrove in 1996 changing into other classes in 2003 in Thailand (left pie chart) and Cambodia (right pie chart). In Trat Province, 60% of the mangrove loss was due to agricultural fields and planted trees, and in Koh Kong Province, 60% of mangroves were replaced by non-mangrove trees. Active and inactive shrimp farms also contribute to the deforestation: 12% in Thailand and 10% in Cambodia.

Figure 4.10 presents the percentage of mangrove deforestation caused by other classes from 2003 to 2009. Similar to Figure 4.9, agricultural and non-mangrove trees are the primary drivers of mangrove deforestation in Thailand from 2003 to 2009. However, the contribution of these two categories decreased in Thailand from 60 % in 2003 to 40 % in 2009. In Koh Kong Province, 70% of mangrove loss was due to non-mangrove trees between 2003 and 2009, which increased by 10% from the previous interval (1996-2003).

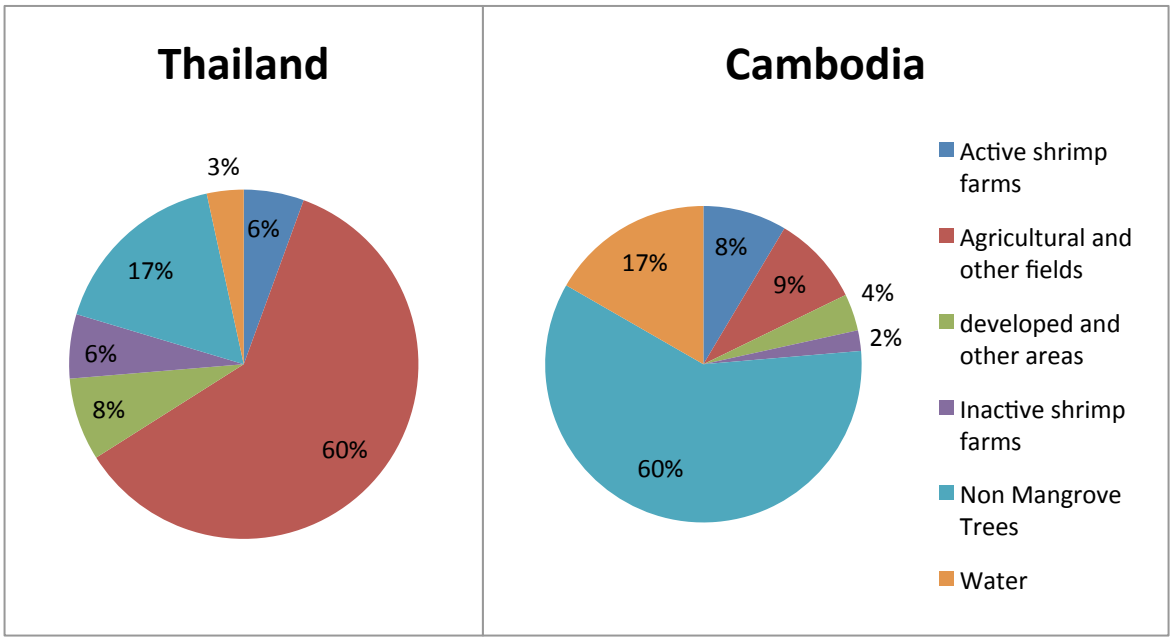

Figure 4.9: Conversion of mangrove area into other land cover/use between 1996 and 2003, in percent.

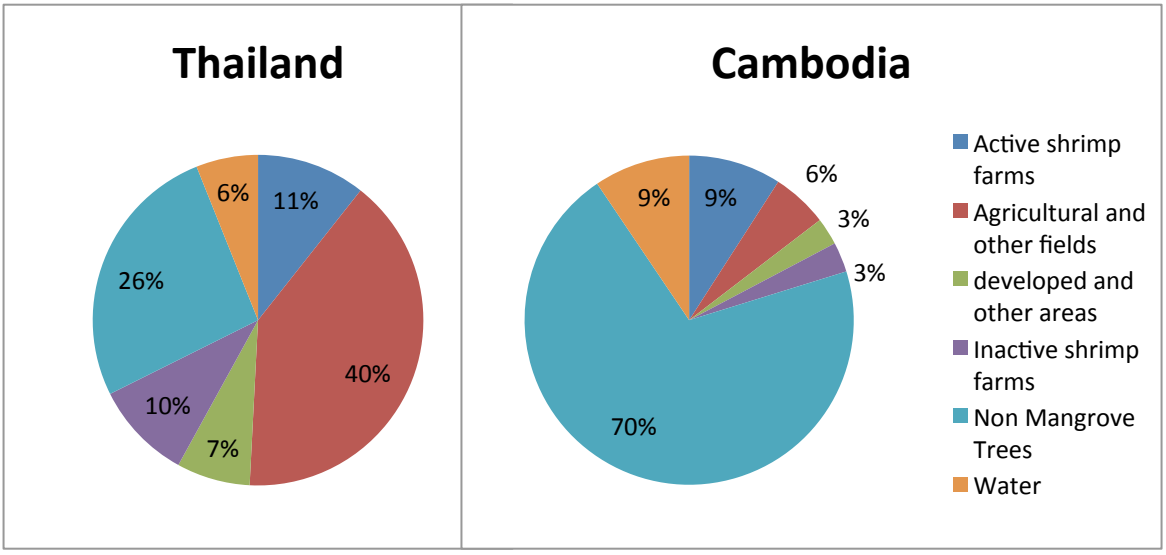

Figure 4.10: Conversion of mangrove area into other land cover/use between 2003 and 2009, in percent.

Active and inactive shrimp farms contribute 21% and 12% in mangrove deforestation in Thailand and Cambodia between 2003 and 2009, respectively (Figure 4.10).

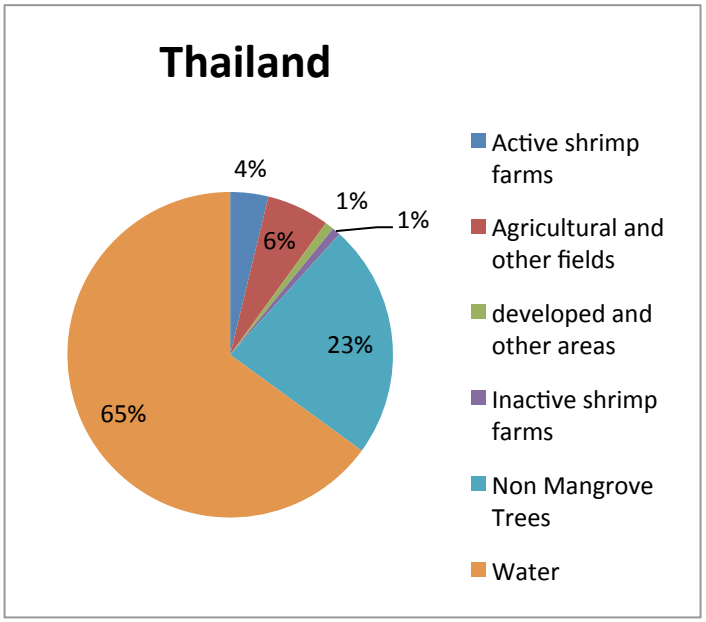

Figure 4.11: Conversion of mangrove area into other land cover/use in Trat Province, Thailand between 2009 and 2015, in percent.

Figure 4.11 shows the percentage of mangrove converted to other classes in Trat, Thailand from 2009 to 2015, where water and non-mangrove trees are the two classes that replaced the mangroves most. The cause of mangrove replacement by water might be flooding or timber collection. Finally, Figure 4.12 shows the percentage of other land cover/use converted into mangroves in Koh Kong Province, Cambodia from 2009 to 2015. This is the only time when mangroves increased by 7.7% from the previous time point. We observed in Figure 4.12 that water and non-mangrove trees are the two main

classes that were replaced by the newly grown mangroves. Our hypotheses on possible causes of growing mangroves are discussed in the Discussion and Conclusion section.

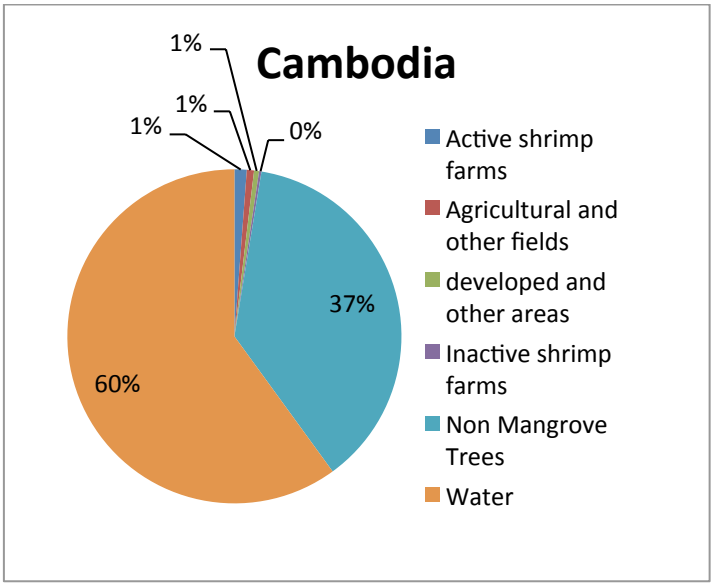

Figure 4.12: Conversion of other land cover/use into mangroves in Koh Kong Province, Cambodia between 2009 and 2015, in percent.

5 DISCUSSION AND CONCLUSIONS

In this research, we used automated classification techniques to identify the total mangrove devastation in the coastal areas of Trat Province, Thailand and Koh Kong Province, Cambodia. Unlike most prior work that used pixel-based image classification for mangrove change detection, we used an object-oriented image analysis procedure with clearly defined steps. We defined seven classes representing land use and land cover types abundant in the areas of our research. Using the classified images from 1996, 2003, 2009, and 2015 we demonstrated how mangroves changed over time in Trat Province and Koh Kong Province. Furthermore, we isolated main drivers in mangrove deforestation in these two areas, which revealed that mangroves were affected by different factors in different geographical locations.

Our image analysis showed that agricultural fields and non-mangrove trees occupied most of the land after mangrove deforestation. The 30m resolution of Landsat was not a high enough resolution to identify planted trees as a separate class. Therefore, planted trees were included either in the agricultural fields or in the non-mangrove trees. We believe that the increase of non-mangrove trees in the coastal buffer is primarily for agricultural and plantation use, including rubber, palm, coconut etc.

Other classes also influenced the deforestation, but their contributions fluctuated in different time periods. We differentiate between active and inactive shrimp farms and study their impact on mangroves separately. This differentiation gave an estimation on

how the shrimp farms changed over the years. Previous work (Aksornkoae *et al.*, 2004, Giri *et al.* 2008, Giri *et al*. 2011) found out that shrimp farms and agricultural fields are the primary driver of mangrove deforestation in our study areas. Our analysis also found that shrimp farms contributed to the deforestation of mangroves in Thailand and Cambodia. However, the impact of shrimp farming is not as severe as was suggested by previous studies.

We observed that mangroves increased by 7.7% from 2009 to 2015 in Koh Kong Province. This observation contrasts with previous years when mangroves consistently decreased over time. Our analysis found that the decrease of active shrimp farms and agricultural fields contributed the most to the growth of mangroves from 2009 to 2015. There is no verified evidence nor published results that we can use to independently verify our finding of increased mangroves in Koh Kong in the recent time. We hypothesize that mangroves appeared to increase because of decreased shrimp firms due to shrimp disease. Further exploratory studies are required to confirm our hypothesis.

There are opportunities for further research and image analysis based on the methodology that we developed. For example, Landsat images have 30mm resolution, which prevented us from detailed exploration of the area where mangrove destruction is the highest and affected the classification accuracy as well. If higher resolution images become available, we can develop a more accurate classifier based on the same methodology. Other shortcomings of our research include image based accuracy assessment. We were not

able to collect field data for accuracy assessment. In our study locations, most of the Landsat images were cloud covered. The Landsat image collected in 1996 was lightly clouded at the southern part of Koh Kong Province. These clouds might have slightly influenced the image classification. We observed that the accuracies of inactive shrimp farms and developed areas were lower than other classes (Table 4.1). Thermal band was used to separate inactive shrimp farms from developed areas as mentioned in Chapter 3. However, the temperature might not have helped significantly to separate these two classes from one another because the images were taken in the morning (9:30 to 10:30 local time).

Mangroves in coastal areas of Thailand and Cambodia are vital to the coastal ecosystem and therefore their protection is badly needed. This research developed a methodology that can be applied to classify and identify change of the classes for freely available Landsat images. The classified images from multiple time points can shed light to the cause of past mangrove deforestation. Based on this information, effective measures can be taken to prevent further damage to precious mangroves. However, further work is needed to identify indirect drivers of mangrove deforestation such as proximity to roads, industry, markets, etc. We also need to consider other global factors impacting mangroves in other countries. One such factor is sea level rise caused by global warming. Incorporating the global and local factors in a single classification model would make it more reliable, which can be used to predict the future more accurately.

References:

Aksornkoae, S., Tokrisna, R., Barbier, E. B., & Sathirathai, S. (2004). Overview of shrimp farming and mangrove loss in Thailand. *Shrimp farming and mangrove loss in Thailand*, 37-51

Beh, B.C., MatJafri, & M.Z., Lim, H.S., (2012). Temporal Change Monitoring of Mangrove Distribution in Penang Island from 2002-2010 by Remote Sensing Approach. *Journal of Applied Sciences,* 12(19), 2044-2051.

Benz, U. C., Hofmann, P., Willhauck, G., Lingenfelder, I., & Heynen, M. (2004). Multiresolution, object-oriented fuzzy analysis of remote sensing data for GIS-ready information. *ISPRS Journal of Photogrammetry and Remote Sensing*, 58, 239–258.

Blaschke, T. (2010). Object based image analysis for remote sensing. *ISPRS Journal of Photogrammetry and Remote Sensing*, 65, 2–16.

Blaschke, T., Lang, S., Lorup, E., Strobl, J., & Zeil, P. (2000). Object-oriented image processing in an integrated GIS/remote sensing environment and perspectives for environmental applications. *Environmental information for planning, politics and the public*, 2, 555-570.

Conchedda, G., Durieux, L., & Mayaux, P. (2008). An object-based method for mapping and change analysis in mangrove ecosystems. *ISPRS Journal of Photogrammetry and Remote Sensing,* 63(5), 578-589.

Congalton, R. G. (1991). A review of assessing the accuracy of classifications of remotely sensed data. Remote sensing of environment,37(1), 35-46.

Congalton, R. G., & Green, K. (2008). *Assessing the accuracy of remotely sensed data: principles and practices*. CRC press.

Dey, V., Zhang, Y., & Zhong, M. (2010). A review on image segmentation techniques with remote sensing perspective. In W. Wagner & B. Székely (Eds.), *ISPRS TC VII Symposium* -100 Years ISPRS (pp. 31–42). Vienna, Austria: IAPRS.

El-Kawy, O. A., Rød, J. K., Ismail, H. A., & Suliman, A. S. (2011). Land use and land cover change detection in the western Nile delta of Egypt using remote sensing data. *Applied Geography*, 31(2), 483-494.

Gao, B. C. (1996). NDWI—A normalized difference water index for remote sensing of vegetation liquid water from space. *Remote sensing of environment*, 58(3), 257-266.

Giri, C., Ochieng, E., Tieszen, L. L., Zhu, Z., Singh, A., Loveland, T., & Duke, N. (2011). Status and distribution of mangrove forests of the world using earth observation satellite data. *Global Ecology and Biogeography,* 20(1), 154-159.

Giri, C., Zhu, Z., Tieszen, L. L., Singh, A., Gillette, S., & Kelmelis, J. A. (2008). Mangrove forest distributions and dynamics (1975–2005) of the tsunami-affected region of Asia. *Journal of Biogeography,* 35(3), 519-528.

Huitric, M., Folke, C., & Kautsky, N. (2002). Development and government policies of the shrimp farming industry in Thailand in relation to mangrove ecosystems. *Ecological Economics*, 40(3), 441-455.

Jackson, T. J., Chen, D., Cosh, M., Li, F., Anderson, M., Walthall, C., Doriaswamy, P., & Hunt, E. R. (2004). Vegetation water content mapping using Landsat data derived normalized difference water index for corn and soybeans. *Remote Sensing of Environment*, 92(4), 475-482.

Ji, L., Zhang, L., & Wylie, B. (2009). Analysis of dynamic thresholds for the normalized difference water index. *Photogrammetric Engineering & Remote Sensing*, 75(11), 1307-1317.

Jianya, G., Haigang, S., Guorui, M., & Qiming, Z. (2008). A review of multi-temporal remote sensing data change detection algorithms. *The international archives of the photogrammetry, remote sensing and spatial information sciences*, 37(B7), 757-762.

Leckie, D. G., Gougeon, F. A., Tinis, S., Nelson, T., Burnett, C. N., & Paradine, D. (2005). Automated tree recognition in old growth conifer stands with high resolution digital imagery. *Remote Sensing of Environment*, 94(3), 311-326.

Mas, J. F. (1999). Monitoring land-cover changes: a comparison of change detection techniques. *International journal of remote sensing*, 20(1), 139-152.

McFeeters, S. K. (1996). The use of the Normalized Difference Water Index (NDWI) in the delineation of open water features. *International journal of remote sensing*, 17(7), 1425-1432.

Myint, S. W., Giri, C. P., Wang, L., Zhu, Z., & Gillette, S. C. (2008). Identifying mangrove species and their surrounding land use and land cover classes using an object-oriented approach with a lacunarity spatial measure. *GIScience & Remote Sensing*, 45(2), 188-208.

Naito, T., & Traesupap, S. (2006). Is shrimp farming in Thailand ecologically sustainable?. *Journal of the Faculty of Economics*, KGU, 16, 55-75.

Nguyen, H. H. (2014). The relation of coastal mangrove changes and adjacent land-use: A review in Southeast Asia and Kien Giang, Vietnam. *Ocean & Coastal Management*, 90, 1-10.

Nguyen, H., McAlpine, C., Pullar, D., Johansen, K., & Duke, N.C. (2013). The relationship of spatial-temporal changes in fringe mangrove extent and adjacent land-use: Case study of Kien Giang coast, Vietnam. *Ocean & Coastal Management*, 76, 12-22.

Peneva-Reed, E. (2014). Understanding land-cover change dynamics of a mangrove ecosystem at the village level in Krabi Province, Thailand, using Landsat data. *GIScience & Remote Sensing,* 51(4), 403-426.

Singh, A. (1989). Review article digital change detection techniques using remotely-sensed data. *International journal of remote sensing*, 10(6), 989-1003.

Song, S.L. (2004). The use of mangroves for aquaculture: Cambodia. In: Promotion of mangrove-friendly shrimp aquaculture in Southeast Asia (pp. 126-130). Tigbauan, Iloilo, Philippines: Aquaculture Department, Southeast Asian Fisheries Development Center.

Vaiphasa, C., De Boer, W. F., Skidmore, A. K., Panitchart, S., Vaiphasa, T., Bamrongrugsa, N., & Santitamnont, P. (2007). Impact of solid shrimp pond waste materials on mangrove growth and mortality: a case study from Pak Phanang, *Thailand. Hydrobiologia*, 591(1), 47-57.